

# Multi-aided Inertial Navigation for Ground Vehicles in Outdoor Uneven Environments

Bingbing Liu<sup>†</sup>, Martin Adams<sup>†</sup>, Javier Ibañez-Guzmán<sup>‡</sup>

<sup>†</sup>*School of Electrical & Electronics Engineering, Nanyang Technological University, Singapore.*

<sup>‡</sup>*SIMTech, 71 Nanyang Drive, Singapore.*

**Abstract**—A good localization ability is essential for an autonomous vehicle to perform any functions. For ground vehicles operating in outdoor, uneven and unstructured environments, the localization task becomes much more difficult than in indoor environments. In urban or forest environments where high buildings or tall trees exist, GPS sensors also fail easily. The main contribution of this paper is that a multi-aided inertial based localization system has been developed to solve the outdoor localization problem. The multi-aiding information is from odometry, an accurate gyroscope and vehicle constraints. Contrary to previous work, a kinematic model is developed to estimate the inertial sensor's lateral velocity. This is particularly important when cornering at speed, and side slip occurs. Experimental results are presented of this system which is able to provide a vehicle's position, velocity and attitude estimation accurately, even when the testing vehicle runs in outdoor uneven environments.

## I. INTRODUCTION

Much effort has been concentrated on solving the famous simultaneous localization and map building (SLAM) problem for mobile robots exploring indoor environments [2],[7],[9]. Contrary to fairly flat and structured indoor environments, it is much more difficult for mobile robots to localize in general outdoor locations. Firstly, wheel encoders suffer much larger systematic errors for heading estimation when the vehicles run on uneven surfaces. Secondly, outdoor environments are often semi-structured or even totally unstructured, which causes feature detection and data association methods [5], [13], widely used in indoor cases, to fail.

A straightforward solution to the problem of localization in outdoor environments is the use of the Global Positioning System (GPS). However the application of GPS is subject to multi-path errors and the problem of limited view of enough satellites, especially in urban or forest areas where high buildings or tall trees exist. Further, GPS can be easily jammed and it maybe totally unavailable, for example, in planetary exploration applications.

Due to the fragile nature of GPS data, more robust methods of localisation need to be found for ground vehicles in outdoor environments. Inertial navigation system are non-jammable and self-contained and can provide pose estimation in 3D due to a triad of orthogonal accelerometers and gyroscopes. Low-cost inertial measurement units (IMUs) are increasingly being made commercially available and the use of INS in automotive applications has increased in the past decade. Since rate information has to be integrated to produce velocity, position and attitude, the

small errors in the rate measurements will cause accumulated unbounded errors in the integrated measurements. Hence, usually IMUs are combined with external sensors to produce effective vehicle pose information.

It is typical to use GPS as the absolute data source to bound INS errors and many INS/GPS navigation systems for autonomous land-borne applications have been developed successfully [14], [15], [16]. Under the consideration that GPS is unavailable, other methods to bound the errors of INS exist in the literature. Barshan *et al* modelled the biases and drifts of inertial sensors as exponential functions of time, and estimated an augmented mobile robot pose state, which contained these bias terms [1]. In [8] and [10], data from odometry and gyroscopes have been fused together for localization. In [11], a method was presented for combining odometry and inertial information to provide an estimate of the six degrees of freedom of a rough terrain rover. Gamini *et al* [6] put forward an on-the-fly alignment method by using the constraints that govern the motion of a vehicle to improve the accuracy of low-cost INS. They made the INS velocities observable by using these constraints and odometric information. Limitations of their method are that the position and attitude are not observable directly. The constraints presented in [6] are often violated in actual applications especially if the vehicle negotiates a bend. In this case side slip, caused by the centripetal forces, is not negligible, and modelling the lateral velocity as Gaussian white noise becomes inadequate.

The main contribution of this paper is that a multi-aided inertial navigation system for outdoor ground vehicles has been developed. Two wheel encoders' data will be fed into a kinematic model to provide the velocity estimate which should be measured by the INS by considering its location on the vehicle. Hence the vehicle's lateral velocity becomes observable and can always be estimated even when it negotiates a turn. An accurate single-axis gyroscope is used to estimate the vehicle's heading angle. The vehicle constraints used in [6] are also used here to make the system more robust. A standard Kalman filter (KF) is adopted to fuse the INS data with the multi-aiding information.

The INS prediction model will be introduced in section II and the multi-aiding method utilising odometry, an additional gyroscope and vehicle constraint information will be presented in section III. In section IV, experimental results, which demonstrate the robust localisation of a utility vehicle, in an outdoor environment, using a lateral

velocity estimator, are shown.

## II. THE INS PREDICTION MODEL

Typical INS sensors contain a triad of orthogonal accelerometers (translatory rate sensors) as well as gyroscopes (angular rate sensors). By integrating the acceleration and angular rate readings from IMU, the autonomous vehicles' pose, that is, the attitude, velocity and position can be computed. In this paper, the objective is to use a multi-aiding method to bound the errors in the estimated INS states. A standard Kalman filter is used to combine the inertial information and the multi-aiding data. The state vector  $\mathbf{X}$  of the KF is:

$$\mathbf{X} = [\delta\mathbf{P}_n^T, \delta\mathbf{V}_n^T, \delta\boldsymbol{\Psi}_n^T]^T \quad (1)$$

where,  $\delta\mathbf{P}_n$ ,  $\delta\mathbf{V}_n$  and  $\delta\boldsymbol{\Psi}_n$  are position, velocity and attitude *error* vectors of the INS in the navigation frame (denoted by subscript  $n$ ) respectively and  $\boldsymbol{\Psi}_n$  consists of  $\gamma, \beta, \theta$ , which are yaw, pitch and roll angles in Euler representation. The state equation is:

$$\dot{\mathbf{X}} = \mathbf{f}(\mathbf{X}, \mathbf{u}) \quad (2)$$

where,  $\mathbf{f}$  will be defined in Eqn. 4. The input is:

$$\mathbf{u} = [\mathbf{A}_b^T, \boldsymbol{\omega}_b^T]^T \quad (3)$$

where,  $\mathbf{A}_b$  and  $\boldsymbol{\omega}_b$  are the acceleration vector and angular rate vector in the body frame<sup>1</sup> (denoted by subscript  $b$ ).

The Pinson error model [12] is used here as the dynamic error propagation model of the INS. That is, the position, velocity and attitude error propagation equations can be written as

$$\begin{aligned} \delta\dot{\mathbf{P}}_n &= \delta\mathbf{V}_n \\ \delta\dot{\mathbf{V}}_n &= \mathbf{A}_n \times \delta\boldsymbol{\Psi}_n + \mathbf{C}_b^n \delta\mathbf{A}_b \\ \delta\dot{\boldsymbol{\Psi}}_n &= -\mathbf{C}_b^n \delta\boldsymbol{\omega}_b \end{aligned} \quad (4)$$

where it should be noted that  $\mathbf{A}_n$  and  $\mathbf{C}_b^n$  are functions of the input vector  $\mathbf{u}$ . In Eqn. 4,  $\delta\mathbf{A}_b$  and  $\delta\boldsymbol{\omega}_b$  are the uncertainties in the accelerometers and gyroscopes in the body frame. These errors can be evaluated accurately when the vehicle is stationary and an initial alignment and calibration has been carried out with the IMU [14], [4]. Hence the state model in Eqn. 4 can be reduced to

$$\begin{bmatrix} \delta\dot{\mathbf{P}}_n \\ \delta\dot{\mathbf{V}}_n \\ \delta\dot{\boldsymbol{\Psi}}_n \end{bmatrix} = \begin{bmatrix} 0 & \mathbf{I} & 0 \\ 0 & 0 & \mathbf{A}_n \times \\ 0 & 0 & 0 \end{bmatrix} \begin{bmatrix} \delta\mathbf{P}_n \\ \delta\mathbf{V}_n \\ \delta\boldsymbol{\Psi}_n \end{bmatrix} = \mathbf{F} \begin{bmatrix} \delta\mathbf{P}_n \\ \delta\mathbf{V}_n \\ \delta\boldsymbol{\Psi}_n \end{bmatrix} \quad (5)$$

where,  $\mathbf{A}_n \times$  is the acceleration in the navigation frame represented in a skew-symmetric form. In Eqn. 5, the bias components of the  $\delta\mathbf{A}_b$  and  $\delta\boldsymbol{\omega}_b$  are assumed to be removed from Eqn. 4 after the initial alignment and calibration and it is further assumed that the remaining components in these error terms can be ignored. The effectiveness of the initial alignment and calibration is shown in [4], where the bias components of the inertial sensors are calibrated by tilt

<sup>1</sup>Please refer to [3] for details on different attitude representations and frames of INS.

sensors when the vehicle is stationary, giving good pose estimation over an extended time.

Eqn. 5 is the fundamental equation that enables the computation of the state  $\mathbf{X}$  of the vehicle from an initial state  $\mathbf{X}(0)$  and the inputs  $\mathbf{A}_b$  and  $\boldsymbol{\omega}_b$ . The process model  $\mathbf{F}$  comprises time-varying terms,  $\mathbf{A}_n \times$ . Thus, numerical methods are used to determine it. Because the update frequency of  $\mathbf{F}$  is much larger than the frequency of the land-borne vehicle's dynamics during the sampling interval  $\Delta t$ , Eqn. 5 can be discretised using the discrete transition matrix  $\mathbf{F}(k)$

$$\begin{aligned} \mathbf{F}(k) &= \exp(\mathbf{F}\Delta t) \\ &= \mathbf{I} + \mathbf{F}\Delta t + \frac{(\mathbf{F}\Delta t)^2}{2!} + \dots \end{aligned} \quad (6)$$

The discretisation is only taken to the first order term since any higher order terms are of negligible value for small  $\Delta t$ .

The discretisation of the state prediction equation can be obtained as

$$\hat{\mathbf{X}}(k|k-1) = \mathbf{F}(k)\hat{\mathbf{X}}(k-1|k-1) \quad (7)$$

Since the acceleration and angular rate input vector  $\mathbf{u}$  affects  $\mathbf{A}_n$  in the process model directly, there is no control vector in the state update equation. The resulting system is linear but  $\mathbf{F}(k)$  must be updated with the input vector  $\mathbf{u}$  at each time step.

The IMU is initially aligned and calibrated by using Nebot's algorithm [4] and all the errors are removed, thus  $\mathbf{X}(1|0)$  is set to zero. However, a corresponding growth in uncertainty in the states due to the drift in the IMU should be evaluated by the predicted covariance matrix

$$\begin{aligned} \mathbf{P}(k|k-1) &= E \left[ (\mathbf{X}(k) - \hat{\mathbf{X}}(k|k-1))(\mathbf{X}(k) - \hat{\mathbf{X}}(k|k-1))^T | \mathbf{Z}^{k-1} \right] \\ &= \mathbf{F}(k)\mathbf{P}(k-1|k-1)\mathbf{F}(k)^T + \mathbf{Q}(k) \end{aligned} \quad (8)$$

This  $9 \times 9$  matrix represents the uncertainty in the IMU predicted errors, in which  $\mathbf{Q}(k)$  is the process noise matrix and  $\mathbf{Z}^{k-1}$  represents all the observation information up to time step  $k-1$ . The observation information will be described in the following section.

## III. MULTI-AIDING INFORMATION FOR INS

The aim of this section is to make a robust INS based navigation system, as depicted in figure 1. The vehicle constraints, used as a "virtual sensor", together with the encoders and a single-axis gyroscope, will be implemented and this subsystem will provide not only velocity observations from the encoders and the "virtual sensor", but also attitude observation from the gyroscope. Hence this multi-aided INS should provide accurate pose predictions for autonomous vehicles. In this section it will be shown how the multi-aiding information can be used to keep the INS errors constrained to a reasonable level.

Under ideal conditions, when the vehicle moves on a surface, it does not slide or leave the ground, which means there is negligible side slip along the lateral direction of the vehicle (y-axis in the body frame) and no motion normal

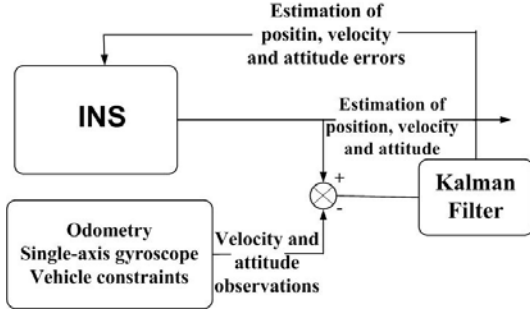


Fig. 1. A multi-aided inertial navigation system. The INS block represents the IMU sensor and the algorithms which carry out the basic inertial computations. The inputs to this block are the Kalman filter estimates.

to the road surface ( $z$ -axis in the body frame) [6]. Thus, reasonable constraints for the vehicle's motion are:

$$\begin{aligned} v_y &= 0 \\ v_z &= 0 \end{aligned} \quad (9)$$

where,  $v_y$  and  $v_z$  are velocities along the  $y$  and  $z$  axes in the body frame respectively.

In practical situations, an approximation can be made to model the constraint violations due to side slip and vibrations caused by the vehicle and road imperfections as follows:

$$v_y = \nu_y \quad (10)$$

$$v_z = \nu_z \quad (11)$$

where,  $\nu_y$  and  $\nu_z$  are Gaussian white noise sources with zero mean and variances  $\sigma_y^2$  and  $\sigma_z^2$  respectively.

In figure 2, the forward velocity  $v_x$  of the IMU along the  $x$  axis in the body frame can also be calculated by using the velocity of the vehicle  $V_r$ , which can be calculated from the wheel incremental encoders directly. Figure 2 presents how the forward velocity  $v_x$  of the IMU is related to the vehicle's forward velocity  $V_r$ .

The vehicle constraints can, however, often be violated, meaning that this model would fail when the vehicle turns, and the side slip is not negligible, which is unavoidable in actual applications. The vehicle would then suffer a considerable lateral velocity and it would therefore not be appropriate to model the side velocity  $v_y$  in the body frame as a white Gaussian noise source. This is especially important when the vehicle has to run in actual urban or forest environments where many sharp turns have to be made. In this section a kinematic model solves this problem by using odometric information to estimate the IMU's body velocities as part of the IMU's kinematic model.

Ideally, an IMU should be mounted exactly at the center of gravity of the vehicle. However, there is usually some offset in actual experiments. In figure 2,  $P$  and  $Q$  define the offset distances of the IMU mounted on the vehicle to the center of the vehicle's rear axle.  $L$  is the length of the vehicle's wheelbase and it is assumed that the actual radii of the vehicle's rear wheels are the same,  $R$ . When

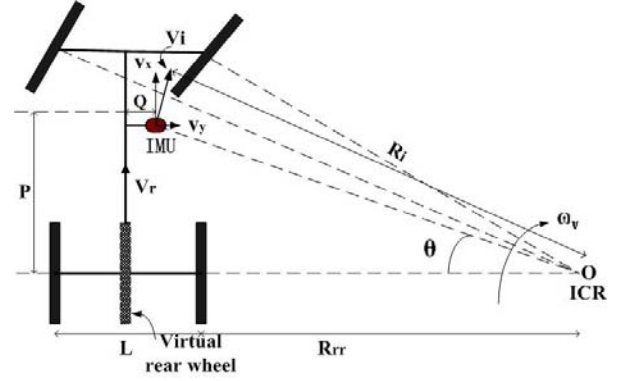


Fig. 2. Vehicle kinematics for a commonly used vehicle with encoders and an IMU.

the vehicle is performing a turn,  $R_{rr}$  and  $R_i$  are the radii of curvature of the path taken by the rear right wheel and the IMU respectively about the instantaneous center of rotation (ICR, denoted by "O" in the figure). According to the assumption that the vehicle is rigid, the angular rate at which any point on the vehicle rotates around "O" is the same,  $\omega_v$ . The forward velocity of the vehicle is  $v_r$  and the velocities in the IMU's body frame along the  $x$  and  $y$  axes are  $v_x$  and  $v_y$  respectively. It is possible to combine the pair of wheels on the rear axle and replace them with a single virtual wheel which lies at the center of the rear axle. The rear left, right and virtual wheels have angular velocities  $\omega_{rl}$ ,  $\omega_{rr}$  and  $\omega_v$  respectively and the first two angular velocities can be calculated from the encoders mounted on the pair of rear wheels directly. The angular velocity of the virtual wheel can simply be calculated as,

$$\omega_r = \frac{1}{2}(\omega_{rl} + \omega_{rr}) \quad (12)$$

By geometry,

$$R_{rr} = \frac{\omega_{rr}L}{\omega_{rl} - \omega_{rr}} \quad (13)$$

Since,

$$V_r = \omega_r R = \omega_v (R_{rr} + \frac{L}{2})$$

$$\omega_v = \frac{\omega_r R}{R_{rr} + \frac{L}{2}}$$

The velocity of the IMU,  $\mathbf{V}_i$  is,

$$\mathbf{V}_i = \omega_v R_i = \frac{\omega_r R}{R_{rr} + \frac{L}{2}} \times \frac{R_{rr} + \frac{L}{2} - Q}{\cos \theta}$$

While  $\theta$  is then given by,

$$\tan \theta = \frac{P}{R_{rr} + \frac{L}{2} - Q}$$

Hence, the velocities in the IMU's body frame along the  $x$  and  $y$  axes,  $v_x$  and  $v_y$  are,

$$v_x = V_i \cos \theta = \frac{\omega_r R}{R_{rr} + \frac{L}{2}} \times (R_{rr} + \frac{L}{2} - Q) \quad (14)$$

$$v_y = V_i \sin \theta = \frac{\omega_r P R}{R_{rr} + \frac{L}{2}} \quad (15)$$

where,  $\omega_r$  and  $R_{rr}$  are defined in Eqns 12 and 13. Hence the observed velocities  $v_x$  and  $v_y$  of the IMU in the body frame, using the information from two encoders mounted on the rear wheels of the vehicle, can be estimated.

Now it is possible to obtain a set of velocities in the body frame by combining  $v_z$  from the “virtual sensor” (Eqn. 11) and  $v_x$  and  $v_y$  from the kinematic model (Eqns. 14 and 15) to calculate the corresponding velocities in the navigation frame. It can be seen that only the velocity sub-state of the state vector

$$\mathbf{X} = [\delta\mathbf{P}_n^T, \delta\mathbf{V}_n^T, \delta\mathbf{\Psi}_n^T]^T$$

is currently observable. In practical operation, when the odometry information is available,  $v_x$  and  $v_y$  are obtained by using Eqns 14 and 15. While at the same time,  $v_z = \nu_z$  is provided by the “virtual sensor”. Hence the velocity observation can be made,

$$\mathbf{z}_V^{velocity}(k) = \mathbf{C}_b^n \begin{bmatrix} v_x(k) \\ v_y(k) \\ v_z(k) \end{bmatrix} = \begin{bmatrix} v_x(k) \cos \beta \cos \gamma + v_y(k) (-\cos \theta \sin \gamma + \sin \theta \sin \beta \cos \gamma) \\ v_x(k) \cos \beta \sin \gamma + v_y(k) (\cos \theta \cos \gamma + \sin \theta \sin \beta \sin \gamma) \\ -v_x(k) \sin \beta + v_y(k) \sin \theta \cos \beta \end{bmatrix} \quad (16)$$

Thus the observation vector of the KF is

$$\mathbf{z}(k) = \mathbf{z}_V^{inertial}(k) - \mathbf{z}_V^{aiding}(k) \quad (17)$$

In order to make the attitude also observable so that the error growth of the INS can be further reduced, an accurate single-axis gyroscope is mounted, aligned with the center line of the vehicle to measure its heading angle. This model is quite simple, in which,

$$\dot{\gamma} = \dot{\Gamma} \quad (18)$$

where,  $\dot{\Gamma}$  is the angular rate reading directly from the gyroscope. It is beneficial to use this accurate single-axis gyroscope to provide the heading observation for the INS if the gyroscope is more accurate than the yaw axis gyro within the INS. As the case here, it is now possible to find commercially available low-cost accurate gyroscopes and the one adopted in our work is a model from KVH, a DSP-5000 fiber optic gyro. The bias level of this model ( $1^\circ/hr$ ) is much smaller than the gyros contained in the IMU ( $5^\circ/hr$ ). Now, based on all the observations, the best estimate for the state vector  $\mathbf{X}$  can be obtained.

When an observation from an aiding sensor, that is the encoders, the “virtual sensor” or the gyroscope, is available, the observation vector is

$$\mathbf{z}(k) = \begin{bmatrix} z_V^{inertial}(k) - z_V^{aiding}(k) \\ z_\gamma^{inertial}(k) - z_\gamma^{gyro}(k) \end{bmatrix} = \begin{bmatrix} (V_T(k) + \delta_V(k)) - (V_T(k) - \nu_V(k)) \\ (\gamma_T(k) + \delta_\gamma(k)) - (\gamma_T(k) - \nu_\gamma(k)) \end{bmatrix} \quad (19) = \begin{bmatrix} \delta_V(k) \\ \delta_\gamma(k) \end{bmatrix} + \begin{bmatrix} \nu_V(k) \\ \nu_\gamma(k) \end{bmatrix}$$

where,  $V_T(k)$  and  $\gamma_T(k)$  are the true values of the velocities and yaw angle and  $\nu_V(k)$  and  $\nu_\gamma(k)$  are noises of the

aiding sensors at time  $k$  respectively. The observation is thus the error between the velocities and yaw angle from the INS and those of the aiding sensors, and the uncertainty in this observation is reflected by the noise of the aiding observation.

Hence the observation matrix is

$$\mathbf{H}(k) = \begin{bmatrix} 0 & 0 & 0 & 1 & 0 & 0 & 0 & 0 & 0 \\ 0 & 0 & 0 & 0 & 1 & 0 & 0 & 0 & 0 \\ 0 & 0 & 0 & 0 & 0 & 1 & 0 & 0 & 0 \\ 0 & 0 & 0 & 0 & 0 & 0 & 1 & 0 & 0 \end{bmatrix} \quad (20)$$

And now the observation equation is

$$\mathbf{z}(k) = \mathbf{H}(k)\mathbf{X} + \boldsymbol{\nu} \quad (21)$$

where  $\boldsymbol{\nu}$  is the observation noise vector, the value of which has been determined experimentally. The updating equations of the KF are standard and omitted here. Once the observations are formed, the state vector can be updated. Hence, the vehicle constraints, odometry and gyroscope can be used to aid the INS to form a robust localization system and produce position, velocity and attitude estimation of the vehicle.

#### IV. RESULTS

In this section, the experimental results will be presented to prove the effectiveness of the multi-aiding method. The testing vehicle is a utility pickup truck. The truck, with all the mounted sensors, is shown in figure 3. The inertial sensor used in this work is a low-cost IMU from Inertial Science, DMARS-I. The IMU together with tilt sensors (for initial calibration) and the single-axis gyroscope were mounted on a rigid platform, which was put on top of the pickup. A digital Honeywell compass was also used to provide the initial heading of the vehicle. The encoders were mounted on the rear wheels as depicted in the figure. A Trimble DGPS was also used in the experiments and the INS/GPS data was fused by using the algorithm in [14]. The INS/GPS result was the best ground truth available, since GPS alone produced large jumps in the estimated vehicle path.

Results from three different kinds of inertial navigation methods, namely the free running INS, the multi-aided INS and the INS/GPS method, are used for comparison.

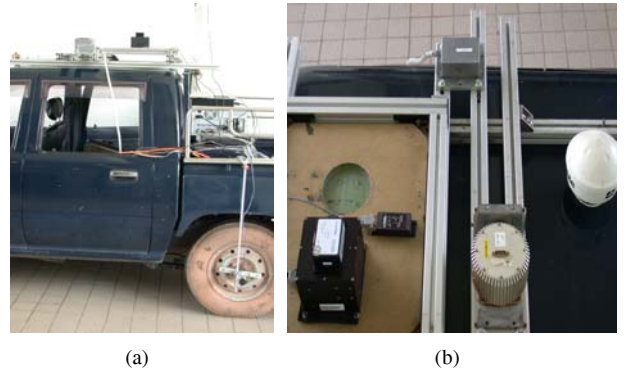


Fig. 3. The testing pickup truck with mounted sensors.

In the experiments, we ran the utility vehicle in an outdoor, undulating environment which is on the campus of Nanyang Technological University. The altitude of this environment ranges from 20 to 50 meters. The whole path is around 1.1 km in length and the vehicle ran for approximately 3 minutes to complete one loop. The map of the environment and the path is shown in figure 4.

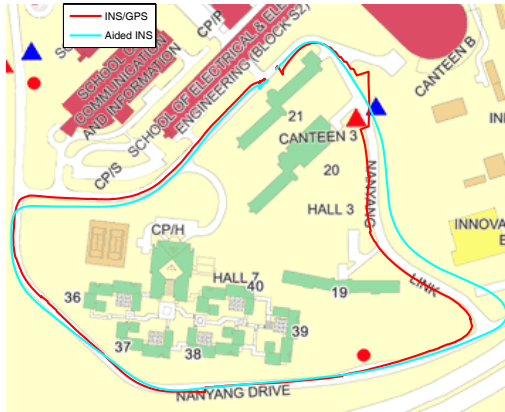


Fig. 4. The testing environment.

In figure 4, the red line shows the path generated from the INS/GPS integration technique, while the cyan line is the path from the multi-aiding method. Compared to the INS/GPS result, the aided INS path was a little offset from the ground truth. Yet, even in the INS/GPS path (assumed to be the ground truth), there were some discontinuities due to the GPS errors. Figure 5 shows the path from the free running INS, compared with the two paths in figure 4. Even after initial calibration, if without any kind of aiding, the free INS can only last for a limited period of time accurately as expected. The mean position errors of the free INS result are 345m and 106m in North and East directions respectively, which are much larger than those of the aided INS, 3.7m and 7.5m.

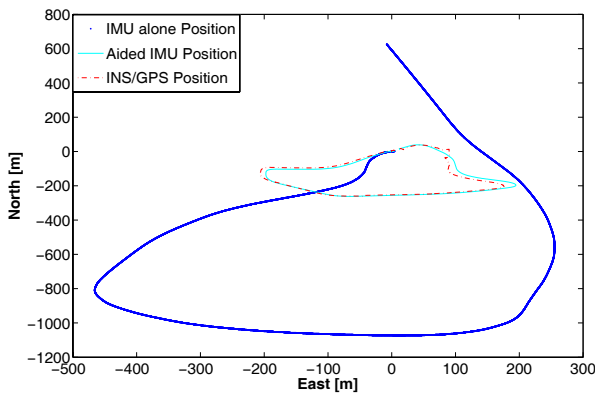


Fig. 5. The generated paths from three methods.

Figure 6 shows the velocity comparison from the 3 different INS methods. The velocities in the north and east directions have been plotted from each method. It is clear that after initial calibration, estimation of velocities from the free running INS soon diverges while the multi-aiding method followed the ground truth well all through the process. The mean velocity errors of the free INS result are 11.6m/s and 6.4m/s in North and East directions respectively, while those of the aided INS are reduced to 0.31m/s and 0.32m/s.

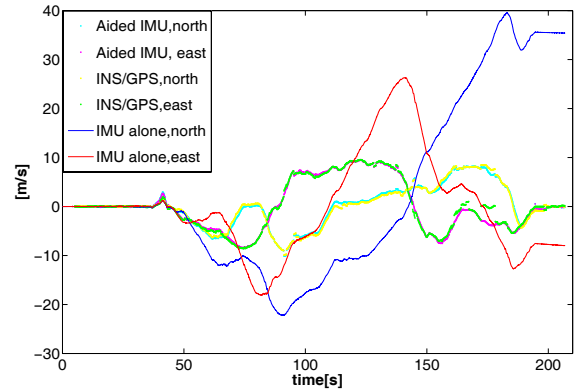


Fig. 6. The comparison of velocities from three methods.

Figure 7 shows the velocity error comparison from the free running INS and the multi-aiding method, using the velocity from the INS/GPS method as the ground truth. The red lines are the  $2\sigma$  error bound of the multi-aiding method, calculated from the appropriate velocity error terms in the estimated error covariances matrix  $\mathbf{P}(k | k)$ .

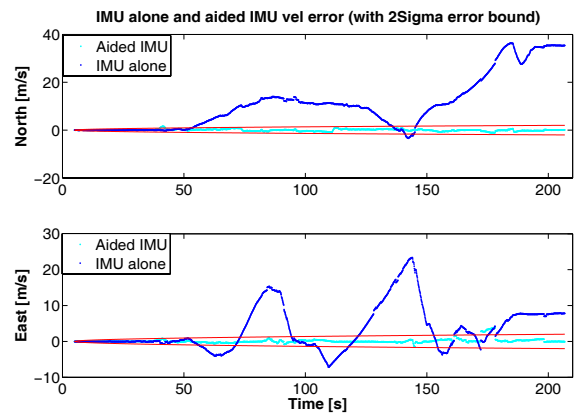


Fig. 7. The comparison of velocity errors from Free INS and Aided INS.

Figure 8 shows the velocities as well as positions in the “down” direction estimated using the 3 different INS methods. Since the vehicle ran in a 3D environment, the pose estimation in this “down” direction is also important. It is seen that the velocity and position estimation from the multi-aiding method follows the INS/GPS estimates much better than those estimated in the free running INS.

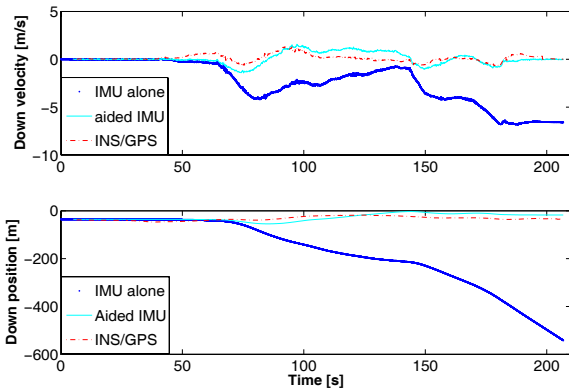


Fig. 8. The comparison of velocities and positions from three methods, in the “down” direction.

In figure 9 the headings of the vehicle from the INS/GPS and the multi-aiding method are shown. Due to the accurate single-axis gyroscope, the heading estimation of the multi-aiding method is relatively accurate. The mean heading error is only  $1.4^\circ$ .

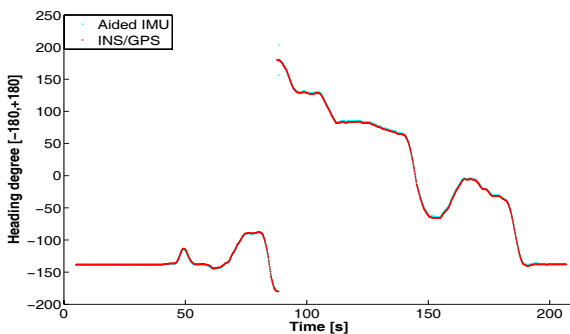


Fig. 9. Comparison of the heading of the vehicle from the INS/GPS integration method and the multi-aiding method.

## V. CONCLUSIONS AND DISCUSSIONS

In this paper, a robust multi-aided inertial based method has been presented for outdoor ground vehicles. The multi-aiding information is from odometry, an accurate single-axis gyroscope and vehicle constraints. A kinematic model has been developed to estimate the inertial sensor’s lateral velocity when cornering is unavoidable within environments. An accurate single-axis gyroscope is used to make the heading estimate observable and hence accurate heading estimate from low-cost IMUs can be achieved. Experimental results from this method have been compared with the standard INS/GPS fusion method and a free running INS method. From the results, it can be seen that even without the help of GPS, the multi-aided INS can still provide reasonable position, velocity and attitude estimation when the testing vehicle operates in outdoor non-flat environments.

In order to make this INS system more robust and accurate, it will be interesting to use GPS as additional

aiding information whenever it is available. In future work, an investigation will be conducted, into which kinds of aiding information, from GPS or from the multi-aiding sensors, should be used to bound the error growth of INS so that the INS can provide the most effective pose estimation accurately and reliably. It will be interesting to add new sensors, for example, an altimeter to the multi-aiding system so that the “down” direction position of the INS can also become observable and the inertial navigation method could improve its accuracy in all directions.

## ACKNOWLEDGMENTS

The authors would like to thank Dr Salah Sukkarieh and Dr Eduardo Nebot from ACFR for their suggestions in the calibration of IMUs. This project has been funded by SIMTech and the second author’s AcRF grant RG10/01, Singapore.

## REFERENCES

- [1] B. Barshan and H.F.Durrant-Whyte, “Inertial navigation systems for mobile robots,” *IEEE Transactions on Robotics and Automation*, vol. 11, no. 3, 1995.
- [2] D. Hahnel, W. Burgard, D. Fox, and S. Thrun, “An efficient fastslam algorithm for generating maps of large-scale cyclic environments from raw laser range measurements,” *Proc. Of Int. Conf. Intelligent Robots and Systems*, 2003.
- [3] D.H.Titterton and J.L.Weston, *Strapdown inertial navigation technology*. Peter Peregrinus Ltd., 1997.
- [4] E. Nebot and H.F.Durrant-Whyte, “Initial calibration and alignment of low cost inertial navigation units for land vehicle applications,” *Journal of Robotics Systems*, vol. 16, no. 2, pp. 81–92, 1999.
- [5] F. Tang, M. Adams, and W.S. Wijesomaand J. Ibanez-Guzman, “Pose invariant, robust feature extraction from range data with a modified scale space approach,” *Proc. Of IEEE International Conference on Robotics and Automation*, 2004.
- [6] G.Dissanayake, S.Sukkarieh, E.M.Nebot, and H.F.Durrant-Whyte, “The aiding of a low-cost strapdown inertial measurement unit using vehicle model constraints for land vehicle applications,” *IEEE Transactions on Robotics and Automation*, vol. 17, no. 5, 2001.
- [7] J.B. Hayet, F. Lerasle, and M. Devy, “A visual landmark framework for indoor mobile robot navigation,” *Proc. Of IEEE International Conference on Robotics and Automation*, 2002.
- [8] J.Borenstein and L. Feng, “Gyrodometry: a new method for combining data from gyros and odometry in mobile robots,” *Proc. Of IEEE International Conference on Robotics and Automation*, 1996.
- [9] J.D.Tardos, J.Neira, P.M.Newman, and J.J.Leonard, “Robust mapping and localization in indoor environments using sonar data,” *Int. J. Robotics Research*, vol. 21, no. 4, pp. 311–330, 2002.
- [10] M. D. Cecco, “Sensor fusion of inertial-odometric navigation as a function of the actual manoeuvres of autonomous guided vehicles,” *Measurement Science and Technology*, vol. 14, pp. 643–653, 2003.
- [11] P. Lamon and R. Siegwart, “Inertial and 3d-odometry fusion in rough terrain - towards real 3d navigation,” *Proc. Of Int. Conf. Intelligent Robots and Systems*, 2004.
- [12] P.Maybeck, *Stochastic Models, Estimation and Control*. Academic Press, 1982, vol. 1.
- [13] S. Zhang, L. Xie, and M. Adams, “An efficient data association approach to simultaneous localization and map building,” *Proc. Of IEEE International Conference on Robotics and Automation*, 2004.
- [14] S.Sukkarieh, E.M.Nebot, and H.F.Durrant-Whyte, “A high integrity imu/gps navigation loop for autonomous land vehicle applications,” *IEEE Transactions on Robotics and Automation*, June 1999.
- [15] Y.Bar-Shalom, X.R.Li, and T.Kirubarajan, *Estimation with Applications To Tracking and Navigation*. Wiley-Interscience, 1998.
- [16] Y.Yang and J.A.Farrell, “Magnetometer and differential carrier phase gps-aided ins for advanced vehicle control,” *IEEE transactions on Robotics and Automation*, 2003.